EMBO reports

scientific report

The tumour suppressor CYLD is a negative regulator of RIG-I-mediated antiviral response

Constantin S. Friedman[1], Marie Anne O'Donnell[1]*, Diana Legarda-Addison[1], Aylwin Ng[2], Washington B. Cárdenas[3], Jacob S. Yount[3], Thomas M. Moran[3], Christopher F. Basler[3], Akihiko Komuro[4,5], Curt M. Horvath[4,5], Ramnik Xavier[2] & Adrian T. Ting[1]*+*

[1]Immunology Institute, Mount Sinai School of Medicine, New York, New York, USA, [2]Center for Computational and Integrative Biology, Massachusetts General Hospital, Boston, Massachusetts, USA, [3]Department of Microbiology, Mount Sinai School of Medicine, New York, New York, USA, [4]Department of Medicine, and [5]Department of Biochemistry, Molecular Biology and Cell Biology, Northwestern University, Evanston, Illinois, USA

On detecting viral RNAs, the RNA helicase retinoic acid-inducible gene I (RIG-I) activates the interferon regulatory factor 3 (IRF3) signalling pathway to induce type I interferon (IFN) gene transcription. How this antiviral signalling pathway might be negatively regulated is poorly understood. Microarray and bioinformatic analysis indicated that the expression of RIG-I and that of the tumour suppressor CYLD (cylindromatosis), a deubiquitinating enzyme that removes Lys 63-linked polyubiquitin chains, are closely correlated, suggesting a functional association between the two molecules. Ectopic expression of CYLD inhibits the IRF3 signalling pathway and IFN production triggered by RIG-I; conversely, CYLD knockdown enhances the response. CYLD removes polyubiquitin chains from RIG-I as well as from TANK binding kinase 1 (TBK1), the kinase that phosphorylates IRF3, coincident with an inhibition of the IRF3 signalling pathway. Furthermore, CYLD protein level is reduced in the presence of tumour necrosis factor and viral infection, concomitant with enhanced IFN production. These findings show that CYLD is a negative regulator of RIG-I-mediated innate antiviral response.

Keywords: cylindromatosis; interferon; IRF3; RIG-I; ubiquitin

EMBO reports (2008) **9**, 930–936. doi:10.1038/embor.2008.136

[1]Immunology Institute, Mount Sinai School of Medicine, Box 1630, One Gustave L Levy Place, New York, New York 10029, USA
[2]Center for Computational and Integrative Biology, Massachusetts General Hospital, 185 Cambridge Street, 7th Floor, Boston, Massachusetts 02114, USA
[3]Department of Microbiology, Mount Sinai School of Medicine, Box 1630, One Gustave L Levy Place, New York, New York 10029, USA
[4]Department of Medicine, and
[5]Department of Biochemistry, Molecular Biology and Cell Biology, Northwestern University, Pancoe Pavilion, Room 4401, 2200 Campus Drive, Evanston, Illinois 60208, USA
*These authors contributed equally to this work
+Corresponding author. Tel: +1 212 659 9410; Fax: +1 212 849 2525; E-mail: adrian.ting@mssm.edu

Received 9 January 2008; revised 18 June 2008; accepted 19 June 2008; published online 18 July 2008

INTRODUCTION

Recognition of virus-derived nucleic acids by the DExD/H-box RNA helicases, the melanoma differentiation-associated gene 5 (MDA5) protein and the retinoic acid-inducible gene I (RIG-I) protein (Yoneyama *et al*, 2005) leads to the production of type I interferon (IFN) in most cell types. Both RIG-I and MDA5 contain caspase recruitment domains (CARDs) that interact with the CARD domain-containing protein interferon-β promoter stimulator 1 (IPS-1), also known as MAVS, VISA or Cardif, which resides on the outer membrane of mitochondria (McWhirter *et al*, 2005). IPS-1, in turn, transduces signals leading to the activation of interferon regulatory factor 3 (IRF3), nuclear factor-kappaB (NF-κB) and activator protein 1 (AP-1) transcription factors (McWhirter *et al*, 2005). IRF3 has a crucial role in antiviral response, as IRF3-deficient mouse embryonic fibroblasts have impaired IFNβ production when infected (Sato *et al*, 2000). IRF3 phosphorylation is mediated by the kinases TANK (TRAF family member-associated NFκB activator) binding kinase 1 (TBK1) and inhibitor-κB kinase ε (IKKε; Fitzgerald *et al*, 2003; Sharma *et al*, 2003). Precisely how IPS-1 activates TBK1 and IKKε remains unclear, and other molecules such as TANK, NEMO/IKKγ and TRAF (TNF receptor-associated factor) family members have also been implicated in the IRF3 signalling cascade (McWhirter *et al*, 2005; Saha *et al*, 2006; Guo & Cheng, 2007; Zhao *et al*, 2007).

The mechanism by which the IRF3 pathway is negatively regulated is poorly understood; however, accumulating evidence suggests that the attachment and removal of polyubiquitin chains might be important. Canonical Lys 48-linked polyubiquitination leads to proteasomal degradation, whereas non-canonical Lys 63-linked polyubiquitination seems to be crucial for signalling (Krappmann & Scheidereit, 2005). A20, a molecule with both E3 ubiquitin ligase and deubiquitinase activity, has been shown to act as a negative regulator of RIG-I-mediated IFNβ gene transcription (Wang *et al*, 2004; Lin *et al*, 2006). RIG-I undergoes Lys 63-linked polyubiquitination (Gack *et al*, 2007), suggesting

that post-translational modification by ubiquitination is probably a crucial mechanism by which the IRF3 pathway can be regulated. Another known deubiquitinase that removes Lys 63-linked polyubiquitin chains is CYLD, a tumour suppressor which was originally identified as a genetic defect in familial cylindromatosis (Bignell *et al*, 2000). CYLD acts as a negative regulator of NF-κB and Jun N-terminal kinase signalling pathways by removing Lys 63-linked polyubiquitin from NEMO/IKKγ, TRAF2 and BCL3 (B-cell CLL/lymphoma3; Brummelkamp *et al*, 2003; Kovalenko *et al*, 2003; Trompouki *et al*, 2003; Massoumi *et al*, 2006). Here, we report that CYLD interacts with components of the RIG-I pathway to inhibit IRF3 signalling and subsequent IFNβ production.

RESULTS AND DISCUSSION

CYLD interacts with RIG-I

Owing to the crucial role of RIG-I in the antiviral response, a search for RIG-I-interacting molecules was performed to uncover regulatory components of the pathway. In particular, molecules that regulate ubiquitination are of interest because of increasing evidence that this post-translational modification has a crucial role in signalling and immune responses (Liu *et al*, 2005). Bioinformatic approaches were initially used to conduct the search. By using gene expression data from 79 human tissues (PMID: 15075390), we examined the tissue- and cell-type expression profiles of 47 genes encoding deubiquitinating enzymes (PMID: 12917690) and 31 genes encoding CARD-containing proteins. Interestingly, both *CYLD* and *RIG-I* (also known as *DDX58*) show a similar expression profile across the 79 tissues and are significantly enriched in immune cells ($P<0.0007$ and $P<0.0002$, respectively, using the Wilcoxon rank-sum test; Fig 1A), suggesting a possible functional association in immune pathways. Furthermore, the analysis of networks constructed from protein interaction data places CYLD and RIG-I within a functional cluster that is important for tumour necrosis factor (TNF) signalling (supplementary Fig 1 online). This computational approach provides a discovery tool to find physical and functional associations between signalling molecules in antiviral responses that have not been previously appreciated.

To confirm the *in silico* analysis, Flag-tagged RIG-I and Myc-tagged CYLD were transfected into 293 Epstein–Barrvirus nuclear antigen (EBNA) cells, and a co-immunoprecipitation experiment was performed (Fig 1B). Myc-tagged CYLD was detected in the anti-Flag immunoprecipitation from cells co-transfected with Flag-RIG-I, but not with a negative control Flag-tagged protein. This observation substantiates the bioinformatics analysis and establishes an interaction between RIG-I and CYLD. To test whether this interaction has functional relevance, the effect of CYLD expression on RIG-I-mediated response was tested by using a synthetic reporter consisting of multimerized PRDI (positive regulatory domain 1) sites derived from the IFNβ promoter that responds to IRF3 activation (Yoneyama *et al*, 1996). Ectopic expression of RIG-I was sufficient to activate the IRF3 reporter, and this response was inhibited by coexpression of CYLD but not of a control protein (Fig 1C). We also observed interaction between endogenous CYLD and RIG-I after infection of 293 EBNA cells with Sendai virus Cantell (SeV; Fig 1D). These data indicate a physical interaction between the two molecules and suggest that CYLD negatively regulates RIG-I and the antiviral response.

CYLD inhibits SeV-induced IFNβ production

To test the above hypothesis, we investigated whether CYLD can modulate the response to SeV infection, which has been shown to trigger IFNβ production in a RIG-I-dependent manner (Kato *et al*, 2005). In control transfected cells, SeV infection induces a robust activation of the IRF3 reporter, but this effect was significantly inhibited in CYLD-transfected cells (Fig 2A). A similar effect of CYLD was observed with a luciferase reporter containing the proximal promoter of IFNβ with binding sites for IRF3, NF-κB and AP-1 (Thanos & Maniatis, 1992; Fig 2A). These reporter assays suggest that CYLD might inhibit IFNβ gene transcription in response to virus infection, which was confirmed by quantitative PCR analysis of IFNβ messenger RNA (Fig 2B). Finally, culture supernatants from infected cells were tested for IFN activity by using a bioassay that measures the ability of IFN to block replication of a green fluorescent protein (GFP)-tagged Newcastle disease virus (NDV). The supernatant from CYLD transfectants infected with SeV inhibited NDV-GFP replication to a lesser extent than the supernatant collected from control transfectants (Fig 2C; supplementary Fig 2A,B online). This indicated that there was less IFN in the CYLD transfectants, which is consistent with the hypothesis that CYLD inhibits RIG-I-mediated IFN production. As a positive control, transfection of the Ebola virus *VP35* gene also inhibited SeV-induced IFN production, as previously reported (Cardenas *et al*, 2006). Cells transfected with CYLD also showed decreased SeV-induced IRF3 and I-kBα phosphorylation (supplementary Fig 2C,D online).

Next, we tested the effect of CYLD loss-of-function using RNA interference. CYLD expression was efficiently knocked down by using a pool of four RNA duplexes (si-CYLD) when compared with control non-silencing oligonucleotides (si-NS; supplementary Fig 3A online). Loss of CYLD expression led to an enhancement in SeV-triggered IRF3 and IFNβ reporters (Fig 2D), phosphorylation of IRF3 and IκBα (supplementary Fig 3C online), and IFNβ mRNA level (Fig 2E). Finally, CYLD knockdown led to enhanced SeV-induced IFN secretion (Fig 2F; supplementary Fig 3B online). Owing to the possibility of off-target effects mediated by the si-CYLD Smartpool duplexes, we used an siRNA duplex that targets the 3′ untranslated region (UTR) of the CYLD mRNA (si-CYLD UTR). The si-CYLD UTR had the same effect as the si-CYLD Smartpool on IFNβ promoter activity, and the effect of the si-CYLD UTR was reversed by co-transfection of the CYLD open reading frame (supplementary Fig 3D online), indicating that the effect of the si-CYLD is not due to an off-target effect. Taken together, these results support the hypothesis that CYLD is a negative regulator of the RIG-I-mediated antiviral response.

CYLD interacts with IPS-1, TBK1 and IKKε

Next, we examined whether CYLD can also interact with other molecules in the RIG-I signalling pathway, as this was suggested from network analysis (supplementary Fig 1 online). Co-immunoprecipitation experiments were performed with the previously identified pathway components IPS-1, TBK1 and IKKε. Myc-tagged CYLD and Flag-tagged RIG-I, IPS-1, TBK1 or IKKε were co-transfected into 293 EBNA cells and, as shown in Fig 3A, CYLD interacted with all of the pathway components tested. Interestingly, the CYLD that coprecipitated with TBK1 and IKKε migrated as a doublet, suggesting that these kinases might be phosphorylating CYLD. However, when the stringency of the immunoprecipited wash buffer was increased from 250 to 500 mM NaCl, the

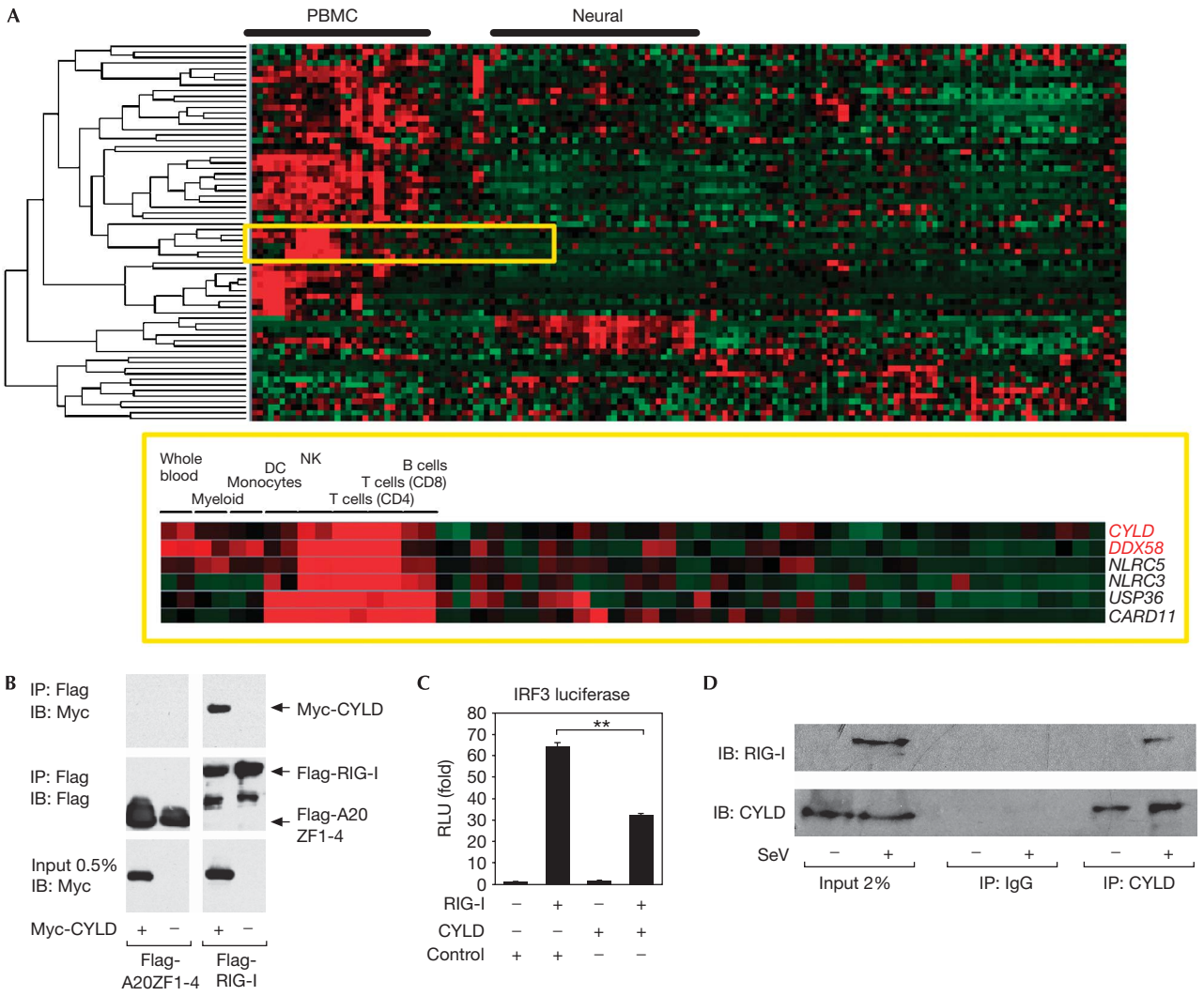

Fig 1 | RIG-I interacts with CYLD *in silico* and functionally. (**A**) Expression profiles of 47 genes encoding DUBs (PMID: 12917690) and 31 genes encoding CARD-containing proteins, across 79 tissues and cell types performed in duplicate. Genes were clustered hierarchically and visualized with TreeView. *CYLD*, a member of the DUB family, and *DDX58* (*RIG-I*), which encodes a CARD-domain-containing protein, clustered closely together on the basis of their similar expression profile overall, and are significantly enriched in immune tissues and cells as found by the Wilcoxon rank-sum test ($P<0.0007$ and $P<0.0002$, respectively). (**B**) A derivative of the 293 EBNA cell line was transfected with 5 μg each of Flag-RIG-I or Flag-A20ZF1-4 as a negative control, and empty vector or Myc-CYLD. Flag immunoprecipitations were performed and sequentially blotted with anti-Myc and anti-Flag. (**C**) IRF3 reporter activity in 293 EBNA cells co-transfected with 100 ng RIG-I and 2 μg of a plasmid encoding CYLD or GST as a negative control. The results are expressed as mean ± s.d. ($n=3$; $^{**}P<0.01$ by Student's *t*-test). (**D**) 293 EBNA cells were infected with SeV at an MOI of 10 for 24 h. Control IgG or anti-CYLD immunoprecipitations were performed and sequentially blotted with anti-RIG-I and anti-CYLD. CARD, Caspase recruitment domain; CD, cluster of differentiation; CYLD, cylindromatosis; DC, dendritic cells; DUBs, deubiquitinating enzymes; GST, glutathione *S*-transferase; MOI, multiplicity of infection; IB, immunoblotting; IP, immunoprecipitation; IRF3, interferon regulatory factor 3; NK, natural killer; PBMC, peripheral blood mononuclear cells; RIG-I, retinoic acid-inducible gene I; RLU, relative luciferase units; SeV, Sendai virus Cantell; siRNA, short interfering RNA; ZF, zinc fingers.

interaction of TBK1 or IKKε with CYLD was no longer observed, suggesting that their interaction with CYLD is weaker than that of RIG-I and IPS-1. To establish a functional role for the observed interactions, we performed an epistasis experiment using the IRF3 and IFNβ luciferase reporters (supplementary Fig 4A–D online). The activation of both reporters by the constitutively active CARD of RIG-I (RIG-IN), IPS-1 and TBK1 was decreased by CYLD in a dosage-dependent manner. However, CYLD did not inhibit the IRF3 response induced by IKKε and seemed to be enhancing it, indicating that CYLD does not globally inhibit all IRF3 response. Similarly, IRF3 phosphorylation induced by overexpression of RIG-IN, IPS-1 and TBK1, but not IKKε, was also blocked by CYLD (Fig 3B). Conversely, CYLD knockdown enhanced the activation of the IRF3 and IFNβ reporters induced by RIG-IN, IPS-1 and TBK1

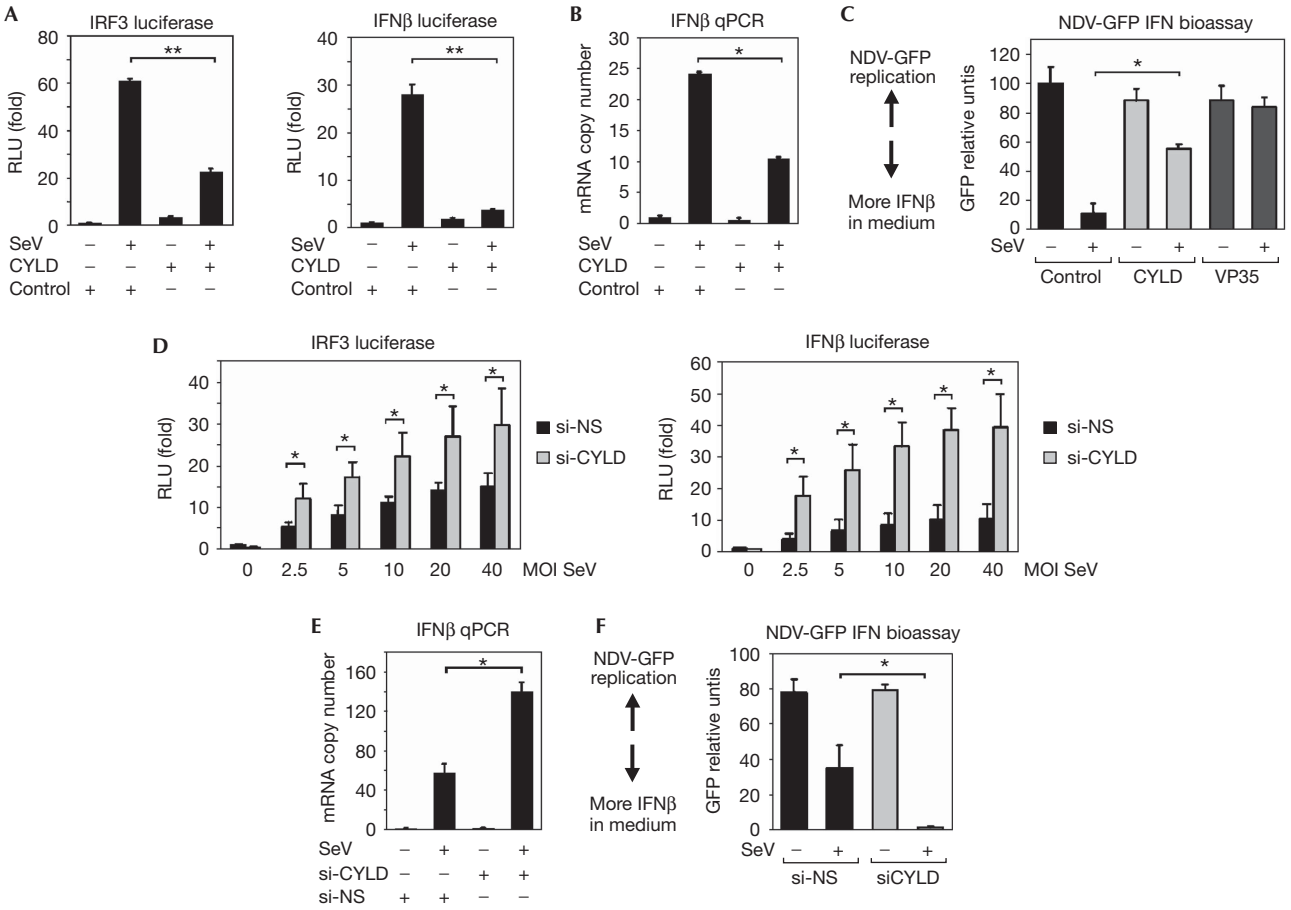

Fig 2 | CYLD inhibits SeV-induced IFNβ production. (**A**) IRF3 and IFNβ promoter activity in 293 EBNA cells transfected with negative control or CYLD, and either mock-infected or infected with SeV at an MOI of 20. The results are expressed as mean ± s.d. ($n = 3$; *$P < 0.05$, **$P < 0.01$ by Student's *t*-test for panels A–F). (**B**) qPCR analysis of IFNβ messenger RNA in 293 EBNA cells transfected with negative control or CYLD, and either mock-infected or infected with SeV at an MOI of 20. (**C**) GFP expression in Vero cells infected with NDV-GFP virus after treatment with conditioned media from cells transfected with 2 μg CYLD, Ebola virus VP35 (positive control) or bacterial GST (negative control) and infected with SeV at an MOI of 10. Higher levels of GFP expression indicate lower levels of IFNβ in the media ($n = 3$). (**D**) IRF3 and IFNβ promoter activity in 293 EBNA cells transfected with siRNA duplexes that are non-silencing (si-NS) or against CYLD (si-CYLD), followed by mock or SeV infection at the indicated MOI. The results are expressed as mean ± s.d. ($n = 4$). (**E**) qPCR analysis of IFNβ mRNA in cells transfected with si-NS or si-CYLD, followed by mock or SeV infection at an MOI of 10. (**F**) IFN bioassay performed with conditioned media from siRNA-transfected cells infected with SeV at an MOI of 20. CYLD, cylindromatosis; GFP, green fluorescent protein; GST, glutathione *S*-transferase; IFN, interferon; IRF3, interferon regulatory factor 3; qPCR, quantitative PCR; MOI, multiplicity of infection; NDV, Newcastle disease virus; SeV, Sendai virus Cantell; siRNA, short interfering RNA.

overexpression, but not by IKKε (supplementary Fig 5 online). The difference in the sensitivity of TBK1 and IKKε to CYLD inhibition is notable in the light of recent studies showing that IKKε is not required for the initial IFNβ induction by virus infection, but is required for the subsequent induction of antiviral genes by IFNβ (Tenoever *et al*, 2007). Thus, these observations are consistent with the idea that several molecules in the pathway, including RIG-I and TBK1, are targets of negative regulation by CYLD.

CYLD deubiquitinates RIG-I, TBK1 and IKKε

The removal of Lys 63-linked polyubiquitin chains from TRAFs and NEMO/IKKγ by CYLD has been shown to inactivate the IKK complex that phosphorylates IκBα (Brummelkamp *et al*, 2003; Kovalenko *et al*, 2003; Trompouki *et al*, 2003). As CYLD inhibits IRF3 signalling induced by RIG-I signalling components, we tested whether these components are targets for CYLD-mediated deubiquitination. 293 EBNA cells were transfected with full-length RIG-I, RIG-IN, IPS-1, TBK1 or IKKε in conjunction with a ubiquitin mutant with only one lysine at position 63 available for conjugation (K63-Ub). Both full-length RIG-I and RIG-IN underwent Lys 63-linked polyubiquitination. TBK1 and IKKε were also modified but to a lesser extent, whereas IPS-1 did not undergo ubiquitination on ectopic expression (Fig 3C). Ubiquitination of RIG-I, RIG-IN, TBK1 and IKKε was abrogated by coexpression of

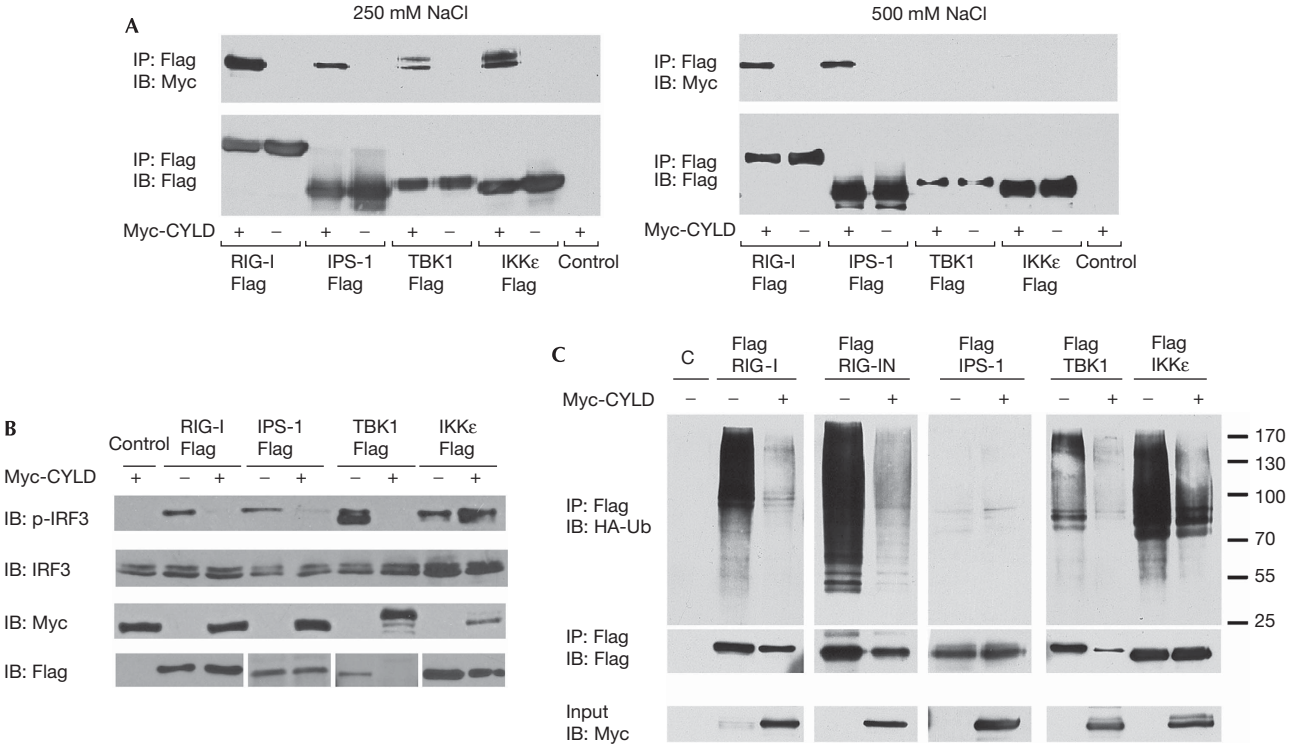

Fig 3 | Physical and functional interactions of CYLD with IPS-1, TBK1 and IKKε. (**A**) Cells were co-transfected with 5 μg of Flag-RIG-I, Flag-IPS-1, Flag-TBK1 or Flag-IKKε and 5 μg of either Myc-CYLD or GST as a negative control. Flag immunoprecipitations were performed, followed by blotting with the indicated antibodies. The washes for the immunoprecipitations were performed in buffer with either 250 mM NaCl (left panel) or 500 mM NaCl (right panel). (**B**) 293 EBNA cells were transfected for 24 h with 1 μg CYLD or empty vector control, and 200 ng each of RIG-I, IPS-1, TBK1 or IKKε. Lysates were blotted for phospho-IRF3 (p-IRF3), total IRF3, Myc-CYLD and Flag-tagged RIG-I, IPS-1, TBK1 or IKKε. (**C**) 293 EBNA cells were transfected with Flag-tagged RIG-I, RIG-IN, IPS-1, TBK1 or IKKε, together with HA-tagged K63-Ub and either empty vector or Myc-tagged CYLD. Triton-soluble lysates were denatured in 1% SDS and immunoprecipitated with anti-Flag. The immunoprecipitations were blotted with anti-HA to detect K63-Ub and re-probed with anti-Flag. The input lysates were blotted with anti-Myc to detect CYLD. CYLD, cylindromatosis; GST, glutathione *S*-transferase; HA, haemagglutinin; IB, immunoblotting; IP, immunoprecipitation; K63-Ub, ubiquitin mutant with a single lysine at position 63; RIG-I, retinoic acid-inducible gene I; TBK1, TANK binding protein 1.

CYLD. A cell-free deubiquitination assay using immuno-affinity-purified Lys 63-polyubiquitinated Flag-RIG-I and CYLD showed that CYLD could directly remove Lys 63 polyubiquitin chains from RIG-I (supplementary Fig 6 online). CYLD inhibits IRF3 signalling induced by RIG-I, IPS-1 and TBK1 (supplementary Fig 4 online), suggesting that ubiquitination is required for RIG-I and TBK1 to activate the IFN response, and that removal of ubiquitin by CYLD inhibits this. Recently, Lys 63-linked ubiquitination of Lys 172 of human RIG-I was reported to be required for RIG-I to associate with IPS-1 to induce IFN (Gack *et al*, 2007); the removal of this modification from RIG-I by CYLD might attenuate the response. The observations that CYLD can deubiquitinate TBK1 and inhibit the IRF3 response induced by TBK1 expression suggest that ubiquitination is also crucial for TBK1 function; however, it is unclear at present how attachment or removal of ubiquitin regulates the enzymatic activity of TBK1. Surprisingly, CYLD consistently reduced the amount of TBK1 protein and, to a lesser extent, that of full-length RIG-I and RIG-IN, whereas levels of IPS-1 and IKKε proteins were relatively unchanged. These observations suggest that the removal of Lys 63-linked polyubiquitin from RIG-I and TBK1 by CYLD might destabilize these molecules, and that this might be another mechanism by which CYLD downmodulates the IFN response.

Regulation of CYLD during infection

Negative regulatory proteins can function as negative feedback molecules to attenuate the response or they can function as 'brakes' that are removed to allow the response to be enhanced. To investigate which of the above mechanisms applies to CYLD, we analysed the CYLD expression level in response to virus infection alone or in conjunction with TNF stimulation. We focused on TNF as a co-stimulus, as the network analysis suggested that TNF is in close proximity to CYLD and RIG-I (supplementary Fig 1 online), and it is known to potentiate IFNβ production triggered by influenza infection (Matikainen *et al*, 2006). TNF alone had no effect on CYLD protein level (Fig 4), in contrast to that reported previously (Jono *et al*, 2004). This discrepancy might be due to a difference in the cell lines used and stimulating conditions. SeV infection alone also had no effect, but infection in the presence of TNF markedly reduced the amount of

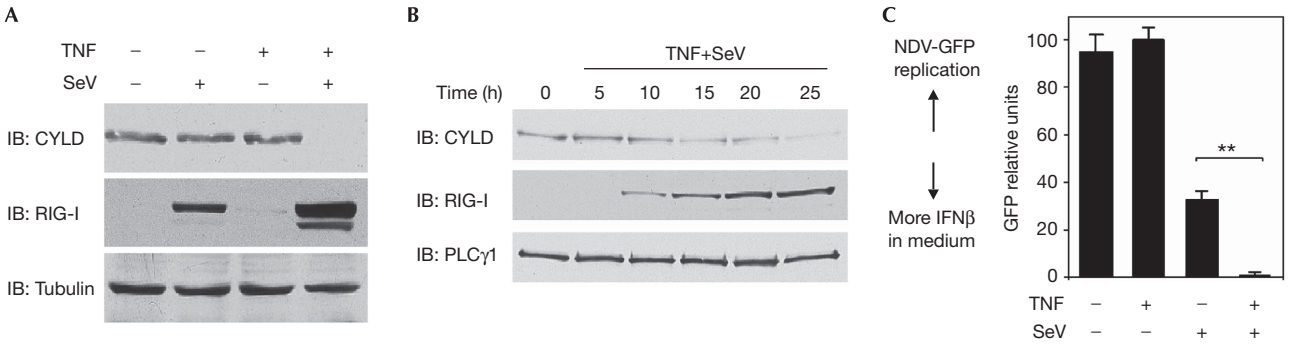

Fig 4 | CYLD protein is downregulated during SeV infection in the presence of TNF. (**A**) 293 EBNA cells were cultured with 25 ng/ml TNF for 24 h before infection with SeV (MOI of 10) for a further 24 h. Triton-soluble lysates were sequentially blotted with antibodies specific for CYLD, RIG-I and tubulin as a loading control. (**B**) Cells were treated with TNF for 24 h before infection with SeV for varying periods of time. Lysates were blotted as indicated. (**C**) Cells were treated as in (**A**), and culture supernatants were collected for IFN bioassay ($n = 3$; $^{**}P < 0.01$). CYLD, cylindromatosis; GFP, green fluorescent protein; IB, immunoblotting; IFN, interferon; MOI, multiplicity of infection; NDV, Newcastle disease virus; PLCγ1, phospholipase C-γ1; RIG-I, retinoic acid-inducible gene I; SeV, Sendai virus Cantell; TNF, tumour necrosis factor.

CYLD protein (Fig 4), coincident with enhanced IRF3 signalling (supplementary Fig 7 online) and IFNβ production (Fig 4). This suggests that CYLD might be reduced as a mechanism to potentiate IFNβ production during viral infection.

In summary, we have shown the inhibitory role of CYLD in regulating type I IFN production during the RIG-I-mediated antiviral response. As IFN upregulates numerous IFN-stimulated genes (ISGs) crucial for antiviral defence, such as ISG15 and ISG56, CYLD probably attenuates the establishment of an antiviral state. The transient inhibition of the activity of CYLD by pharmacological agents might therefore provide a strategy to enhance antiviral responses.

METHODS

Analysis of gene expression across 79 tissues. Microarray data files were obtained from the Novartis GNF human expression atlas version 2 resource (PMID: 15075390), and expression values of 33,689 probe sets from the HG-U133A (Affymetrix, Santa Clara, CA, USA) platform and the GNF1H custom chip were analysed. The data set was normalized by using global median scaling and we filtered the data by excluding from the analysis probe sets with 100% 'absent' calls (MAS 5.0 algorithm) across all 79 tissues. The data set was further filtered by setting a minimum threshold value >20 in at least one sample for each probe set and a maximum mean expression value >100. Hierarchical clustering (complete linkage method) was performed with Cluster 3.0 using Pearson's correlation as the similarity metric. *Z*-score transformation was applied to each probe set across all arrays before generating 'heatmaps' for visualization using TreeView.

Interferon bioassay. The IFN bioassay was performed as described previously (Cardenas *et al*, 2006). Conditioned supernatants (100 μl) from SeV-infected cells were subjected to ultraviolet irradiation to inactivate infectious SeV and overlaid onto Vero cells seeded in a 96-well black microtitre plate (Costar, Cambridge, MA, USA). After 24 h, the Vero cells were infected with the IFN-sensitive virus NDV-GFP for 1 h at an MOI (multiplicity of infection) of 6 in serum-free media. At 24 h after infection, GFP fluorescence was quantified in a FLUOstar OPTIMA plate reader (BMG Labtechnologies, Offenburg, Germany) set with excitation and emission wavelengths at 485 and 530 nm, respectively. The relative GFP unit for each sample was calculated using the formula (value of sample−value of background)/(value of highest sample−value of background) × 100.

Co-immunoprecipitation of endogenous proteins. A total of 1×10^8 293 EBNA cells per sample were mock or SeV infected for 24 h and then lysed in an ice-cold buffer containing 1% CHAPS (3-[(3-cholamidopropyl)dimethylammonio]-1-propanesulfonate), 50 mM Tris, 150 mM NaCl, 5 mM $MgCl_2$, pH 7.5 supplemented with protease inhibitors. Lysates were clarified by centrifugation at 10,000*g* at 4 °C and incubated for 2 h with 1 μg of CYLD antibody or normal mouse IgG. Immune complexes were precipitated for 30 min at 4 °C with 2.5 μl of protein A/G beads pre-blocked with BSA. Beads were washed three times with 1% CHAPS lysis buffer and then boiled in SDS sample buffer. Samples were resolved on SDS–PAGE and analysed by sequential blotting with anti-RIG-I and anti-CYLD.

***In vivo* deubiquitination assay.** Flag-tagged RIG-I signalling molecules were co-transfected with haemagglutinin-tagged Lys 63-Ub, and either vector or Myc-CYLD. After 24 h, cells were incubated with 25 μM MG132 for 4 h and then lysed in Triton lysis buffer. Lysates were denatured with 1% SDS at 100 °C for 5 min, immunoprecipitated with anti-Flag beads, eluted with Flag peptide and immunoblotted.

Additional methods are described in the supplementary information online.

Supplementary information is available at *EMBO reports* online (http://www.emboreports.org).

ACKNOWLEDGEMENTS

We thank C. Lopez for her critical reading of the manuscript and S.-C. Sun, A. Garcia-Sastre, J. Hiscott, D. Thanos, J. Chen and T. Fujita for providing crucial reagents. This paper is dedicated to the memory of the late P. Leibson, whose passion for science, teaching and life remains a great inspiration to many others (A.T.T.). This study was supported in part by National Institutes of Health (NIH) grants AI052417 (A.T.T.), AI057997 (A.T.T.), AI059536 (C.F.B.), AI041111 (T.M.M.), AI062623 (T.M.M.), AI073919 (C.M.H.) and AI062773 (R.X.). C.S.F.

was supported in part by the NIH T32 AI07647-Training Program: Mechanisms of Virus–Host Interactions. M.A.O'D. and A.N. are recipients of Research Fellowship Awards from the Crohn's and Colitis Foundation of America. W.B.C. was supported in part by a fellowship awarded through grant AI057158 (Northeast Biodefense Center-Lipkin). D.L.-A. is supported by an NIH Ruth L. Kirschstein NRSA Postdoctoral Award AI065058. A.T.T. is a recipient of the Irma T. Hirschl Career Scientist Award.

CONFLICT OF INTEREST

The authors declare that they have no conflict of interest.

REFERENCES

Bignell GR *et al* (2000) Identification of the familial cylindromatosis tumour-suppressor gene. *Nat Genet* **25:** 160–165

Brummelkamp TR, Nijman SM, Dirac AM, Bernards R (2003) Loss of the cylindromatosis tumour suppressor inhibits apoptosis by activating NF-κB. *Nature* **424:** 797–801

Cardenas WB, Loo YM, Gale M Jr, Hartman AL, Kimberlin CR, Martinez-Sobrido L, Saphire EO, Basler CF (2006) Ebola virus VP35 protein binds double-stranded RNA and inhibits α/β interferon production induced by RIG-I signaling. *J Virol* **80:** 5168–5178

Fitzgerald KA, McWhirter SM, Faia KL, Rowe DC, Latz E, Golenbock DT, Coyle AJ, Liao SM, Maniatis T (2003) IKKε and TBK1 are essential components of the IRF3 signaling pathway. *Nat Immunol* **4:** 491–496

Gack MU *et al* (2007) TRIM25 RING-finger E3 ubiquitin ligase is essential for RIG-I-mediated antiviral activity. *Nature* **446:** 916–920

Guo B, Cheng G (2007) Modulation of the interferon antiviral response by the TBK1/IKKi adaptor protein TANK. *J Biol Chem* **282:** 11817–11826

Jono H, Lim JH, Chen LF, Xu H, Trompouki E, Pan ZK, Mosialos G, Li JD (2004) NF-κB is essential for induction of CYLD, the negative regulator of NF-κB: evidence for a novel inducible autoregulatory feedback pathway. *J Biol Chem* **279:** 36171–36174

Kato H *et al* (2005) Cell type-specific involvement of RIG-I in antiviral response. *Immunity* **23:** 19–28

Kovalenko A, Chable-Bessia C, Cantarella G, Israel A, Wallach D, Courtois G (2003) The tumour suppressor CYLD negatively regulates NF-κB signalling by deubiquitination. *Nature* **424:** 801–805

Krappmann D, Scheidereit C (2005) A pervasive role of ubiquitin conjugation in activation and termination of IκB kinase pathways. *EMBO Rep* **6:** 321–326

Lin R, Yang L, Nakhaei P, Sun Q, Sharif-Askari E, Julkunen I, Hiscott J (2006) Negative regulation of the retinoic acid-inducible gene I-induced antiviral state by the ubiquitin-editing protein A20. *J Biol Chem* **281:** 2095–2103

Liu YC, Penninger J, Karin M (2005) Immunity by ubiquitylation: a reversible process of modification. *Nat Rev Immunol* **5:** 941–952

Massoumi R, Chmielarska K, Hennecke K, Pfeifer A, Fassler R (2006) Cyld inhibits tumor cell proliferation by blocking Bcl-3-dependent NF-κB signaling. *Cell* **125:** 665–677

Matikainen S *et al* (2006) Tumor necrosis factor α enhances influenza A virus-induced expression of antiviral cytokines by activating RIG-I gene expression. *J Virol* **80:** 3515–3522

McWhirter SM, Tenoever BR, Maniatis T (2005) Connecting mitochondria and innate immunity. *Cell* **122:** 645–647

Saha SK *et al* (2006) Regulation of antiviral responses by a direct and specific interaction between TRAF3 and Cardif. *EMBO J* **25:** 3257–3263

Sato M *et al* (2000) Distinct and essential roles of transcription factors IRF-3 and IRF-7 in response to viruses for IFN-α/β gene induction. *Immunity* **13:** 539–548

Sharma S, tenOever BR, Grandvaux N, Zhou GP, Lin R, Hiscott J (2003) Triggering the interferon antiviral response through an IKK-related pathway. *Science* **300:** 1148–1151

Tenoever BR, Ng SL, Chua MA, McWhirter SM, Garcia-Sastre A, Maniatis T (2007) Multiple functions of the IKK-related kinase IKKε in interferon-mediated antiviral immunity. *Science* **315:** 1274–1278

Thanos D, Maniatis T (1992) The high mobility group protein HMG I(Y) is required for NF-κ B-dependent virus induction of the human IFN-β gene. *Cell* **71:** 777–789

Trompouki E, Hatzivassiliou E, Tsichritzis T, Farmer H, Ashworth A, Mosialos G (2003) CYLD is a deubiquitinating enzyme that negatively regulates NF-κB activation by TNFR family members. *Nature* **424:** 793–796

Wang YY, Li L, Han KJ, Zhai Z, Shu HB (2004) A20 is a potent inhibitor of TLR3- and Sendai virus-induced activation of NF-κB and ISRE and IFN-β promoter. *FEBS Lett* **576:** 86–90

Yoneyama M, Suhara W, Fukuhara Y, Sato M, Ozato K, Fujita T (1996) Autocrine amplification of type I interferon gene expression mediated by interferon stimulated gene factor 3 (ISGF3). *J Biochem* **120:** 160–169

Yoneyama M *et al* (2005) Shared and unique functions of the DExD/H-box helicases RIG-I, MDA5, and LGP2 in antiviral innate immunity. *J Immunol* **175:** 2851–2858

Zhao T, Yang L, Sun Q, Arguello M, Ballard DW, Hiscott J, Lin R (2007) The NEMO adaptor bridges the nuclear factor-κB and interferon regulatory factor signaling pathways. *Nat Immunol* **8:** 592–600